Response for Reviewer #1:

Comment to “Measurement Report: Aircraft observations of secondary ice production in convective clouds over the Tibetan Plateau”

This study makes a useful contribution to the observational literature on SIP, particularly in the under-sampled Tibetan Plateau region. The finding of an extended SIP temperature window and the emphasis on droplet size thresholds are potentially important for model parameterization. However, the heavy reliance on a single flight day for process-level conclusions, the uncertainty surrounding INP estimation in a pristine environment, and the tentative nature of mechanism attribution need to be more rigorously addressed.

Reply: In response to the valuable comments from you and the other reviewers, the manuscript has been thoroughly revised. We accept the central criticism: the earlier manuscript attributed enhanced ice concentrations to specific SIP mechanisms (HM, DS, BR) on the basis of local, Eulerian measurements, which cannot support such attribution. The objective of the paper has therefore been changed rather than merely softened. The study now aims to show the observational signatures of ice enhancement consistent with SIP in convective clouds over the TP, to examine how these signatures vary with temperature and with the concentrations of hydrometeors that can act as SIP partners, and to state explicitly what the dataset can and cannot resolve. Mechanism names are retained only as descriptions of particle assemblages ("consistent with"), and the alternatives of vertical transport and of several possible coexisting mechanisms are stated wherever cold-level enhancement is discussed.

The manuscript has been revised mainly as follows:

(1) The meteorological context has been expanded. Fig. 2 now includes distributions of the FY-2D visible image, brightness temperature (TBB), ground-based radar reflectivity and the Naqu sounding profile (wind, temperature, 0°C level, LCL, CCL).

(2) The round (drizzle) concentration has been recalculated from $0.9 \leq C < 1.2$ and $D \geq 90$ μm, following the 50-pixel shape threshold of Taylor et al. (2016), and all figures and statistics involving round particles have been redrawn.

(3) The term "SIP ratio" has been removed. The metric is now the IMF=N_{ice}/N_{INP}, attributed explicitly to Field et al. (2017) and Wieder et al. (2022), with Nice restricted to irregular particles ($N_{ice}=N_{irreg}$). The uncertainty of the parameterized INP concentration and the limitations of the IMF methodology have been now discussed in Sect. 4.2.

(4) ERA5 vertical velocity fields (Horizontal distribution and vertical cross-section, Fig. 15) have been added, and the upward transport of secondary ice is now discussed as an alternative explanation that the data cannot exclude. In addition, a habit census by temperature bin in case 4 has been added (Fig. 13i).

(5) HVPS spectra have been added to Figs. 10 and 14, so that the ice, drizzle and large-particle spectra are now presented over the full 2DS10 to HVPS range.

(6) We have redrawn Figure 16 to discuss the relationship between ice concentration enhancement and the concentrations of drizzle ($D \geq 90$ μm) and large hydrometeors (HVPS, $D \geq 300$ μm) across different temperature intervals.

(7) Table 3 and Sect. 4.1 have been substantially expanded, covering the Northern Hemisphere, the

Southern Hemisphere and the tropics.

We believe the revised manuscript is a more defensible contribution: it documents the ice enhancement, its temperature range, its spectral signature and its association with large droplets and hydrometeors.

General comments

(1) While the statistical analysis in Section 3.3 draws on seven flights, the detailed process-level investigation (cases 1–5, size thresholds, and mechanism attribution) relies almost entirely on a single flight on 6 July 2014. The authors acknowledge this limitation in Section 4.2, but it remains a significant caveat. The convective regime on that day may not be representative of all summer convective clouds over the TP.

Reply: We have restructured the manuscript. In Section 3.1, we first provide an overview of the background conditions over the TP based on the aerosol and cloud microphysical characteristics from seven flights (Fig. S1), namely low aerosol concentrations ($N_{500} < 10$ cm^{-3}) but relatively high ice crystal concentrations, with a maximum exceeding 200 L−1. Against this background, we selected one well-sampled flight with high data quality (20140706) for detailed analysis in Sections 3.2 and 3.3, to investigate the in situ observational evidence associated with ice enhancement and its dependence on environmental conditions. In addition, we have added a discussion of the limitations of a single-case study in Section 4.2.

Lines 566-582:

A fundamental limitation of this study is that both the observational evidence for the ice enhancement and the analysis of particle spectral evolution rest primarily on a single well-observed flight case (06 July 2014). This case was selected because it exhibited the most comprehensive microphysical observations and the strongest SIP signatures, allowing for a robust process-level analysis. Although only this case is analyzed in detail, it comprises five segments (cases 1–5) that collectively cover a range of conditions. Robust evidence of ice enhancement was found in several consecutive legs. In the warm layers of cases 1, 2 and 4, the particle observations were consistent with HM. In case 4, continuous vertical profiling showed that the enhancement persisted across the sampled temperature range, down to −16°C. Case 3 provides the contrasting test. Large droplets were present within the HM temperature range, yet no SIP signature was detected, and graupel and other large ice-phase hydrometeors were absent from the same layers. Conversely, case 5, sampled at −16°C, indicates that SIP may also occur at low temperatures when drizzle and large hydrometeors are present. Collectively, these consistent and contrasting observations support an association between high ice concentrations over the TP and SIP, and further suggest that the enhancement was accompanied by favorable temperature conditions, as well as sufficient graupel and large hydrometeors. Nonetheless, because the 06 July case represents a specific convective regime under clean aerosol conditions, quantitative values (e.g., the drizzle size of about 200 μm at cold levels and the 1 L^{-1} thresholds used in Sect. 3.3) and the relative contributions of specific SIP mechanisms may not be universally applicable to all cloud types or environmental conditions over the TP. Future campaigns with more extensive sampling across diverse convective regimes are needed to further validate and refine these findings.

(2) The SIP ratio is central to this study, yet the INP concentrations are estimated using the DeMott et al. (2010) parameterization, which was developed from mid-latitude and marine data. The TP is characterized by extremely clean aerosol conditions (N_{500} < 10 cm^{-3}) over complex topography, and recent studies suggest that global parameterizations can substantially overestimate INP in such pristine high-altitude environments (while I am not sure about the influence of topography). The authors briefly note this in Section 4.2, but the implications deserve more thorough treatment.

Reply: We have re-estimated the INP concentrations, as shown in Fig. 5c. Between −2 and −20°C, the INP concentrations were below or near to 1 L^{-1}.

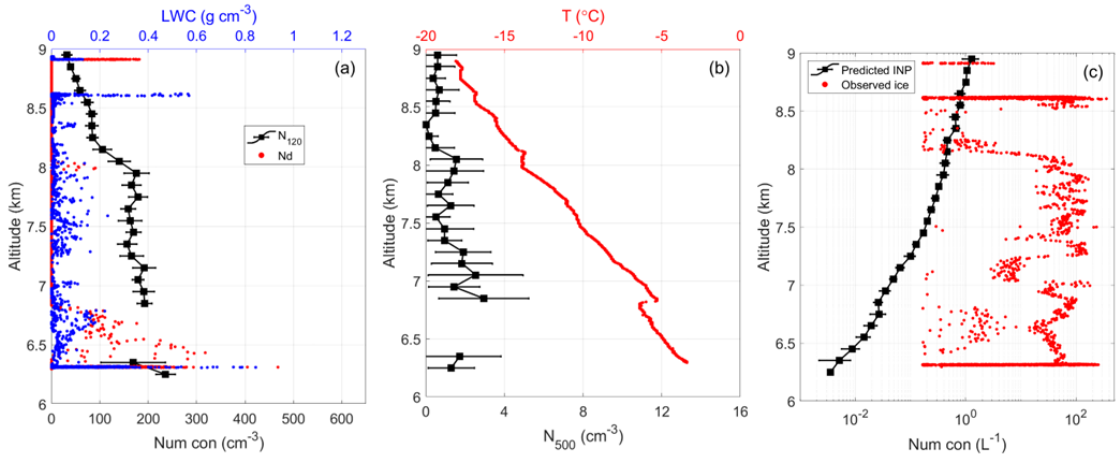

Figure 5: Vertical profiles on 6 July 2014: (a) cloud droplet number concentration from FCDP (N_d, red scatters), LWC from Hotwire (blue scatters) and average aerosol number concentration with size larger than 120 nm (N_{120}, black scatters); (b) temperature (red scatters) and average aerosol number concentration with size larger than 500 nm (N_{500}, black scatters); (c) the concentrations of predicted INP (black line) and observed ice (red scatters).

We have expanded the discussion on the estimation uncertainty of INP concentrations in Sections 2.3 and 4.2.

Lines 135-147:

INP play a crucial role in primary ice formation within clouds, thereby influencing cloud microphysics and precipitation processes (Hoose and Möhler, 2012; Kanji et al., 2017). Recent precipitation-based measurements reported INP concentrations over the TP of 0.002 to 0.675 L^{-1} between −7.1°C and −27.5°C, comparable to those in the Arctic and lower than typical mid-latitude continental values (Chen et al., 2021). Since direct measurements of INP were not available during the TIPEX-III campaign, the empirical parameterization of DeMott et al. (2010) was adopted to infer INP concentrations (N_{INP}). The same scheme has been applied to pristine Antarctic air, where it still performed better than many other available parameterizations, although it was not perfectly applicable (Grosvenor et al., 2012). Accordingly, the N_{INP} (L^{-1}) was estimated from the concentration of aerosols with size larger than 0.5 μm ($N_{a,0.5}$, cm^{-3}) sampled outside clouds:

$$N_{INP} = a(273.16 - T)^b \left(N_{a,0.5}\right)^{c(273.16-T)+d} \quad (1)$$

where T is temperature (K), a = 0.0000594, b = 3.33, c = 0.0264, and d = 0.0033. Therefore, aerosol loading exerts a much weaker influence on N_{INP} than temperature: over the temperature range −2 to

−30°C, N_{INP} varies by approximately four orders of magnitude, whereas even a tenfold increase in $N_{a,0.5}$ alters N_{INP} by less than one order of magnitude at any given temperature.

Lines 598-614:

A further source of uncertainty concerns the estimation of INP concentrations. The IMF used in this study relies on the empirical parameterization of DeMott et al. (2010), which was developed from mid-latitude and oceanic data and may not fully represent the unique low-aerosol environment of the TP, especially at low temperatures (Sect. 2.3). Moreover, given that the clean background aerosol concentrations over the TP are substantially lower than those used in the DeMott parameterization development, the estimated INP concentrations are likely overestimated in this study, implying that the reported IMF should be considered as conservative lower bounds of the actual ice enhancement. Additionally, the complex topography of the TP can modulate aerosol vertical transport and spatial distribution (Tan et al., 2021; Zhou et al., 2024), adding further uncertainty to INP estimates. Even if N_{INP} were measured directly, the IMF would remain a diagnostic of ice enhancement rather than a measure of SIP efficiency, because it compares in-cloud ice of both primary and secondary origin with the INP concentrations inferred from aerosol sampled outside cloud, and thus requires that the two describe the same air mass and that no primary ice has been lost since nucleation (Korolev et al., 2020). Values below unity therefore indicate an inconsistency between the estimate and the observed ice population rather than the absence of SIP, and the ratio cannot be converted into a number of secondary ice crystals per primary INP. Despite these limitations, the observed ice enhancement and its environmental dependences are robust and provide useful constraints for improving microphysical parameterizations in high-altitude cloud models. These findings also highlight the urgent need for in situ INP measurements over the TP, particularly at temperatures below −10°C, to refine SIP efficiency assessments and to develop region-specific INP parameterizations.

(3) The attribution of HM, DS, and BR relies on indirect evidence (particle habits, temperature ranges, and coexistence of hydrometeor types). While this is a common challenge in observational SIP studies, the authors should be more cautious in their descriptions. For example, for Case 3 (−4°C, no graupel or columnar crystals), DS is inferred because large droplets (>50 μm) are present. However, without direct imaging of droplet fragmentation, this remains speculative. For temperatures below −8°C, the persistence of columnar crystals is interpreted as evidence of upward transport from the HM zone. An alternative explanation is that columnar crystals can grow at temperatures down to roughly −10°C (Bailey & Hallett, 2009), so their presence alone does not require vertical transport. Please clarify why upward transport is the preferred explanation.

Reply:

① **Correction regarding the inference of DS in case 3**

We have revised the speculation regarding DS in case 3.

Lines 280-284: However, case 3 was sampled within the same temperature range (approximately −4°C) but showed none of these signatures. The cloud was liquid-dominated, ice concentrations remained below 10 L^{-1} (Fig. S4e), and neither columnar crystals nor graupel were detected (Fig. S5), although the drizzle concentrations reached up to 20 L^{-1} (Fig. S4b). A plausible explanation is that the absence of rimed particles (or graupel) may have limited efficient HM despite the presence

of large droplets.

Lines 322-325: In contrast, although case 3 lay within the HM temperature regime and contained relatively large droplets (up to 200 μm), the HVPS probe detected no particles exceeding 1000 μm and graupel or other large hydrometeors were absent, so that the conditions for SIP were not met. Consequently, the ice crystal spectra of case 3 did not display the pronounced bimodal structure seen in cases 1 and 2.

② **Identifying the source of columnar crystals at low temperatures**

We statistically analyzed the proportions of ice crystal habits within different temperature ranges in case 4 (Fig. 13i) and found that columnar ice crystals in the layer warmer than −8 °C were nearly twice as abundant as those in the cold layer. Therefore, columnar ice crystals do not dominate in the cold layer. We suggest that these columnar ice crystals were mainly secondary ice generated in the warm layer and carried to the cold layer by updrafts (based on ERA5, Fig. 15), thereby causing the ice enhancement. Of course, other local SIP processes may also occur in the cold layer. However, with the current data, it is very difficult to separate these two processes. A detailed analysis has now been added in Sect. 3.2.2 of the manuscript (Lines 396-427):

Finally, one question remains unresolved: where did the columnar crystals detected at the cold levels come from? According to the habit diagram of Bailey and Hallett (2009), columnar habits form mainly at temperatures warmer than about –10°C, so their presence at 8–8.6 km (down to –16°C) is not readily explained by primary growth at those temperatures and instead points to a source region at warmer levels. Secondary production of columnar crystals at these temperatures is no more plausible than primary growth, because columnar crystals are the characteristic product of HM and splintering is efficient only within the –3 to –8°C window (Hallett and Mossop, 1974). Griggs and Choularton (1983) further suggested that rimed droplets freeze so rapidly below –8°C that the resulting ice shell becomes too rigid to splinter. Taylor et al. (2016) offered a transport-based explanation for their presence at cold levels: although columnar crystals are an expected product of HM splintering mainly within the –3 to –8°C range, they can also be observed at other temperatures when displaced by updrafts and downdrafts. Their occurrence at cold levels therefore may point to vertical transport from the warm layer. Moreover, the column class was about twice as abundant in the warmer bins (about 6.5–7.8%) as in the colder bins (about 3.4–4.3%), consistent with preferential production in the warm HM layer and subsequent transport to the cold levels. The ERA5 vertical-velocity fields in Fig. 15 provide a first-order test of this transport pathway. In the horizontal distributions, broad regions of upward motion were present over and around the case 4 domain at 450, 400 and 350 hPa (about 6.6, 7.5 and 8.5 km; Figs. 15a–f), and the updraft signal extended up to 350 hPa. The vertical cross-sections along 31.75°N (Figs. 15g and 15h) show coherent upward motion across the 6–9 km layer, linking the warm HM layer near 6.3 km to the cold sampling height near 8.6 km. This upward motion was more pronounced at 11:00 than at 10:00, with 11:00 being the case 4 sampling time. Such sustained updrafts offered a natural pathway for lofting columnar crystals from lower (warmer) levels to the cold levels below –10°C, a process that Korolev et al. (2020, 2024) showed can supply secondary ice to substantially colder cloud layers. The columnar crystals at cold levels are therefore better explained by upward transport from the warmer HM layers than by local formation, although a minor locally produced contribution cannot be excluded from the crystal habits alone.

The observations presented here also shed light on the cold-level ice enhancement in case 4. Primary nucleation alone cannot account for it, since the ice concentrations at these levels exceeded

the N_{INP} by two to three orders (−8 to −13°C) and by one to two orders near −16°C (Fig. 12). A plausible supply is the upward transport of secondary ice from the warmer HM layers, which would by itself raise the ice concentration at cold levels (Korolev et al., 2020, 2024). In-situ SIP within the cold layer, however, may contribute as well, since supercooled large droplets and large hydrometeors persisted below –10°C (Figs. 11 and 14), providing conditions favorable for SIP. Part of the needle class may consist of fine fragments produced locally by BR. The particle populations required by such pathways were likewise present in the cold layer: graupel remained the most abundant large hydrometeor below –13°C (about 9%, Fig. 13i), and dendritic crystals, although few in number, were still present, so the dense and the fragile particle types whose collisions are invoked in the BR process were both available. The drizzle that persisted below –10°C likewise provided the supercooled large droplets required by droplet-shattering pathways. However, we cannot quantify the vertical transported versus locally secondary ice formed fractions based on present dataset.

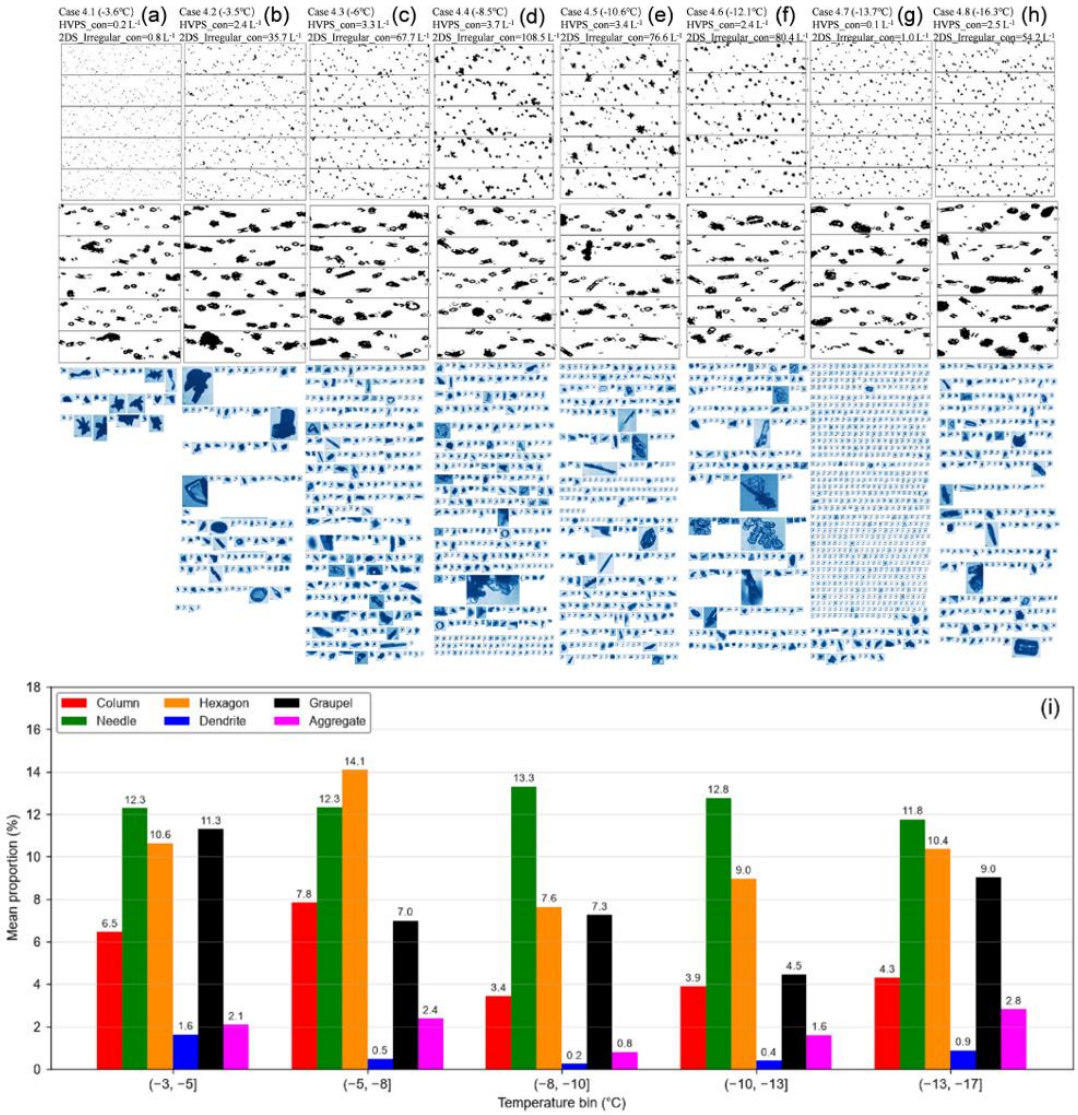

Figure 13: Example images (a–h) of 2DS and CPI from −3.6 to −16.3°C in case 4; values at the top of each image indicate average temperature and particle concentration. (i) Mean relative abundances of six ice crystal habit classes as a function of temperature in case 4, binned into intervals of (−3, −5], (−5, −8], (−8, −10], (−10, −13], (−13, −17] °C. Habits were classified from 2DS10

images into eight classes; the six ice habits (column, needle, dendrite, hexagon, aggregate and graupel) are shown, whereas broken and spherical particles are omitted, so the six series do not sum to 100%.

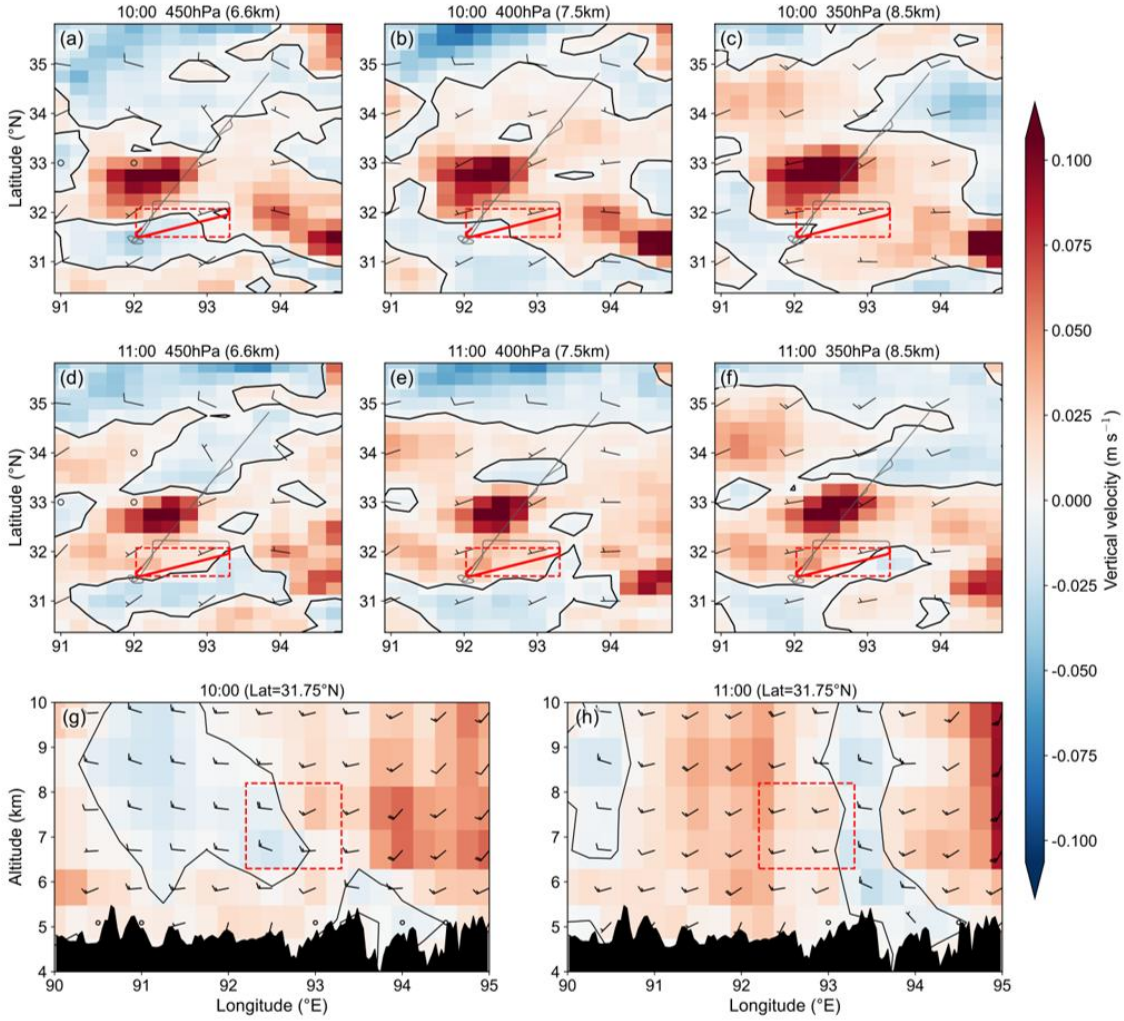

Figure 15. ERA5 vertical velocity (m s^{-1}, upward positive) over the flight region on 6 July 2014: horizontal distributions at 450/400/350 hPa for 10:00 (a–c) and 11:00 (d–f), and vertical cross-sections along 31.75°N for 10:00 (g) and 11:00 (h). Black contours are $w = 0$; barbs show horizontal wind (cross-sections: u and w×100). Gray/red lines are the full track and case 4 segment (11:15–11:40); red dashed boxes mark the case 4.

(4) The BR mechanism is invoked several times, but direct observational evidence (e.g., images of freshly broken crystal fragments with matching habits) is not explicitly shown. The authors should either provide more direct imaging evidence or temper their claims about BR's contribution relative to DS at low temperatures.

Reply: We have reselected the CPI images for Fig. 9. Unfortunately, because a considerable amount of CPI image data is missing, no images that effectively support the DS mechanism have been found so far. Therefore, in this manuscript, we can only make reasonable inferences and discussion regarding the existence of the DS at different temperatures based on temperature, ice concentrations, round concentrations, and some CPI images. The discussion of the DS and BR mechanisms in the text has also been weakened.

Lines 285–301:

In addition to the HM process, the CPI images in Fig. 9 further exhibit particle features that are morphologically consistent with other possible SIP mechanisms. Dendritic snowflakes were clearly present in cases 1 and 2, and were inferred to have formed at higher (colder) levels and to have sedimented into this layer. The CPI images highlighted by green boxes show broken branches and detached fragments adjacent to fragile dendritic snowflakes, features that are morphologically consistent with BR. Collisional breakup of ice particles near –5°C has been documented to produce fine needles and columnar fragments (Hou et al., 2023; Knight, 2012). Korolev and Leisner (2020) also noted that BR is most likely in mixed-phase convective regions. Therefore, these fragments in Fig. 9 could potentially originate from the collisional breakup of dendritic snowflakes. However, no observational technique can determine whether such fragments originated from the BR process within the cloud or from shattering upon interaction with the probe itself, and similar detachments may also arise from other mechanical processes. Furthermore, the supercooled droplets in Fig. 9 marked by red boxes have small fragments in their immediate vicinity, a morphology that could result from the freezing and subsequent fragmentation of droplets. Identifiable fragmentation products of the type used in previous studies (Lawson et al., 2015, 2017; Korolev et al., 2020) to infer active droplet shattering are not clearly evident in these images, and comparable morphologies may also arise from other processes such as HM or probe shattering. Overall, the present interpretation is based solely on limited CPI images and carries considerable uncertainty, but we cannot rule out contributions from SIP mechanisms other than HM to the ice enhancement observed in cases 1 and 2.

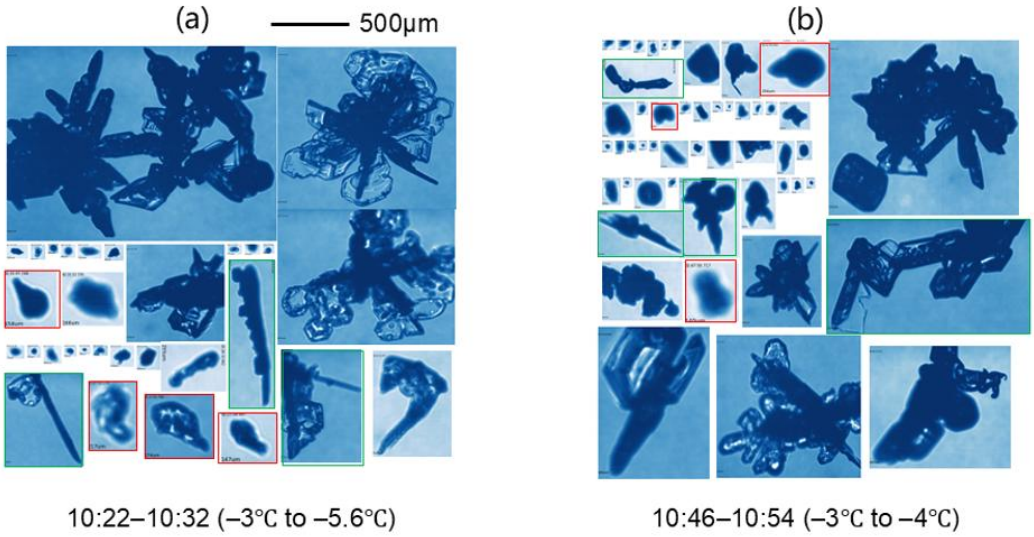

Figure 9: Example CPI images of panel (a) case 1 and panel (b) case 2.

Detailed comments

Line 33-36, two sentences could be merged into one.

Reply: We have revised as follows (Lines 35-37): The most widely studied process is the Hallett–Mossop (HM) process, also known as rime splintering, in which ice particles collide with supercooled droplets during riming at –3°C to –8°C, producing numerous small columnar ice crystals (Hallett and Mossop, 1974; Mossop, 1985).

Line 38-39, Recent studies could also be mentioned, such as Li et al. (2024, doi: 10.1016/j.atmosres.2024.107288).

Reply: We have added this reference as follows (Lines 39-40): In addition, the interaction between seeder-feeder and the HM processes from −3℃ to −6℃ has been observed in convective clouds during the MeiYu season (Li et al., 2024).

Section 2.1, Uncertainties associated with aircraft observations should be described or discussed, particularly over the TP.

Reply: We have revised Section 2.1, adding and discussing the uncertainties in aircraft observations.

Lines 102-105: For imaging probes, the choice of maximum dimension definition can alter derived number concentrations by up to a factor of 6, and different data processing algorithms applied to the same raw dataset can yield concentrations differing by nearly two orders of magnitude (McFarquhar et al., 2017).

Lines 112-118: Different choices in data processing algorithms for airborne in situ observations can lead to uncertainties in derived cloud microphysical parameters (McFarquhar et al., 2017). Over the TP, the complex terrain and rapidly developing convective clouds may further magnify these statistical uncertainties. Nevertheless, previous studies in this region have largely depended on remote sensing and ground-based measurements, leaving in situ cloud microphysical observations notably sparse. Aircraft observations therefore remain the most direct and effective approach for depicting cloud microphysical characteristics in this high-altitude area. Despite these limitations, the consistency of our key findings across independent flight legs and missions lends support to the robustness of our principal conclusions.

Line 98, LWC and IWC should be defined first before they are used.

Reply: The full names of LWC and IWC were first introduced with their abbreviations in the Introduction (Section1, Lines 63-66): Using ground-based millimeter cloud radar, unimodal distributions of both ice and liquid cloud microphysical properties were identified over the TP, with distinct relationships between ice effective radius, ice water content (IWC), and temperature in high-level ice clouds, as well as increasing trends of droplet effective radius and liquid water content (LWC) with height in low-level liquid clouds (Zhao et al., 2016, 2017).

Therefore, the abbreviations are already defined prior to their use in Section 2.1. To avoid repetition, IWC and LWC are used directly in Section 2.1.

Line 109-113, Reliability of support of the phase classification method should be provided or discussed.

Reply:

(1) We have added three supporting references for the classification between ice clouds and water clouds (Ke et al., 2024; Korolev et al., 2003; Wu et al., 2022). The subdivision of water clouds is primarily based on droplet size. The revised text is as follows (Lines 128-133):

Cloud phase was classified from the IWC-to-LWC ratio and the particle categories. Samples with IWC/LWC > 10 and irregular particle concentrations from 2DS10 more than 10 L^{-1} were classified as ice cloud (Ke et al., 2024; Korolev et al., 2003; Wu et al., 2022). The remaining samples were classified as liquid water cloud. Based on droplet size, with 20 μm as the condensation–coalescence transition (Jonas, 1996), the liquid water clouds were subdivided into small water cloud

(maximum droplet diameter smaller than 20 μm), large water cloud (round particle concentrations from 2DS more than 10 L^{-1}), and middle water cloud (all remaining liquid water samples).

(2) In addition, we have corrected the calculation of drizzle concentrations following the method of Taylor et al. (2016). Lines 122-127:

For particles smaller than about 90 μm (about 50 pixels), however, shape-based phase discrimination is unreliable and tends to inflate the apparent round (liquid) concentration. Adopting the same practice as Taylor et al. (2016), shape classification was performed on all particles, but the 90 μm threshold was applied to the round class only. Particles with $0.9 \leq C < 1.2$ and $D \geq 90$ μm were therefore classified as round particles (drizzle), whereas smaller circular particles were grouped into a non-phase-discriminated "small" category. In addition, images with $C \geq 1.2$ were classified as irregular particles (ice).

Figure 3, I wonder why there are no droplet with diameters larger than 20 um for small water clouds, which is kind of weird to me for clouds over relatively clean environment over the TP.

Reply: As defined in Section 2.2, clouds with a maximum droplet diameter smaller than 20 μm are classified as small water clouds in our study. Accordingly, the droplet effective diameter shown in Fig. 3a is 9.3 μm. In field observations, it is physically reasonable for shallow cloud layers to exhibit droplet effective diameters below 20 μm, as the limited vertical development and short residence time restrict the activation and growth of collision-coalescence processes. This does not contradict the clean background of the TP, but rather reflects the substantial inhomogeneity of cloud microphysical properties across different stages of cloud development.

Line 193, “with in” should be “within”

Reply: We have revised as follows (Lines 252-254): In case 1.1 (about −5.6°C), the cloud was dominated by large cloud droplets within updraft regions, with drizzle concentrations exceeding 20 L^{-1}. The LWC derived from FCDP reached up to 0.5 g m^{-3} (Fig. 7c), while ice number concentrations remained below 10 L^{-1}.

Figure 9, a legend regarding the size could be helpful.

Reply: We have added a legend regarding the size (500 μm) in Fig. 9 as follows:

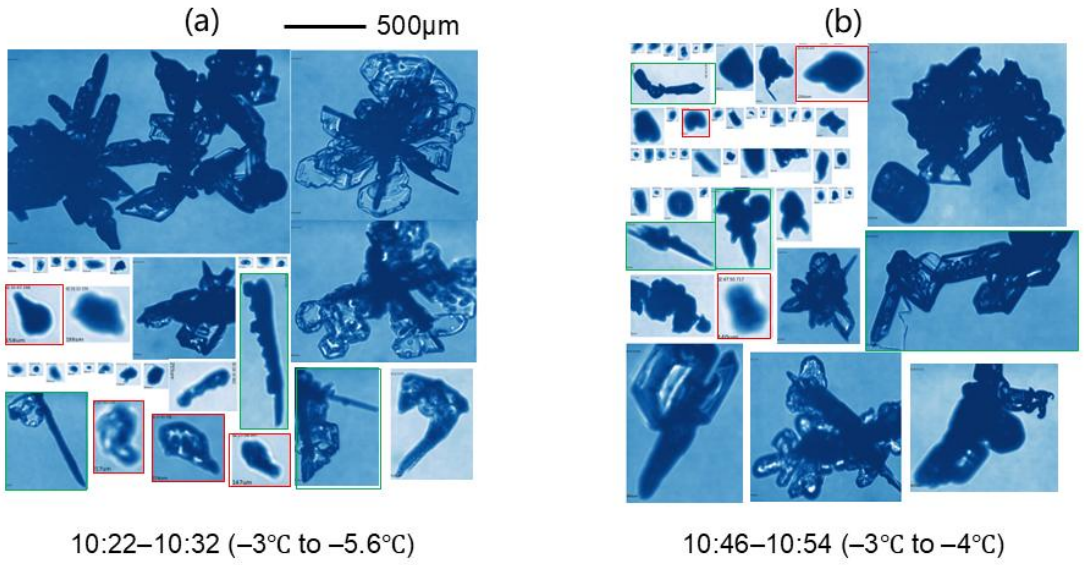

Figure 9: Example CPI images of panel (a) case 1 and panel (b) case 2.

Line 243-244, Why not both?

Reply: We have revised the manuscript and deleted this sentence.

Fig. 10: The dotted grey lines in panels (a), (c), and (e) need a legend entry. Are these extrapolated or smoothed fits?

Reply: We thank the reviewer for pointing out this ambiguity in our figure presentation.

We would like to clarify that all curves in Figures 10 and 14 (original 15) are purely observational data, and no extrapolation, smoothing, or fitting has been applied. The "dotted grey lines" noticed by the reviewer are not a separate dataset, nor are they fitting results. Rather, they are an artifact of the step-plot representation used to display binned size distribution data: when a particular size bin contains zero measured concentration, the plotting routine naturally breaks the line segment, creating a visual gap. When such gaps occur across consecutive sparse bins, the line appears fragmented and visually resembles a "dotted" or "dashed" line.

To eliminate this ambiguity, we have revised the caption of Figures 10 and 14 as follows:

Figure 10: Mean size distributions (step plots) of (a1–a3) irregular particles from 2DS, (b1–b3) round droplets (drizzle) from 2DS, and (c1–c3) all particles from HVPS for cases 1–3. Different coloured lines represent selected legs within each case.

Figure 14: Mean size distributions (step plots) of ice particles (left), round droplets (drizzle, center) from 2DS and all particles(right) from HVPS: (a, b, c) case 4 and (d, e, f) case 5. Different coloured lines represent selected legs within each case.

Line 252-255, Is the finding applicable to other cases over other locations? More general conclusion is appreciated. If not, a short discussion could be helpful. Also, "Droplet size controls SIP initiation" — this is a strong causal statement. Since the study is observational, consider softening to "Droplet size appears to be the controlling factor for SIP initiation" or similar.

Reply: We agree with your suggestions. It is not rigorous to draw such a strong causal statement based on a single observation. We have removed this statement from the manuscript.

Lines 386-392:

In summary, the images and spectra demonstrate that across the full –3.6 to –16.3°C range the ice population was a temperature-dependent mixture whose bimodal size structure was the spectral signature of ice enhancement, and that at low temperatures the controlling factor for SIP initiation may be the presence of sufficiently large supercooled droplets (about 200 µm). The observed drizzle size reached about 200 µm, the size at which DS is most efficient in laboratory experiments and in the parameterization (Phillips et al., 2018; Lauber et al., 2021). If these round particles were still liquid at −16°C, their subsequent freezing would fall in this size range, and DS cannot be excluded as a contributor to the ice enhancement at this temperature.

Figure 15, Why are the droplet size with maximum values around 300 um?

Reply: We acknowledge that the maximum droplet diameter observed in the spectra reaches approximately 300 µm. However, our study focuses on the spectral peak diameter rather than the absolute maximum size. As clearly shown in Fig. 14 (original Fig. 15), the legs that exhibit a pronounced spectral peak near 200 µm correspond well with the ice-enhanced legs, whereas such a spectral feature is absent in the other legs. This reinforces our conclusion that the presence of a droplet spectral mode near 200 µm, rather than the absolute maximum size.

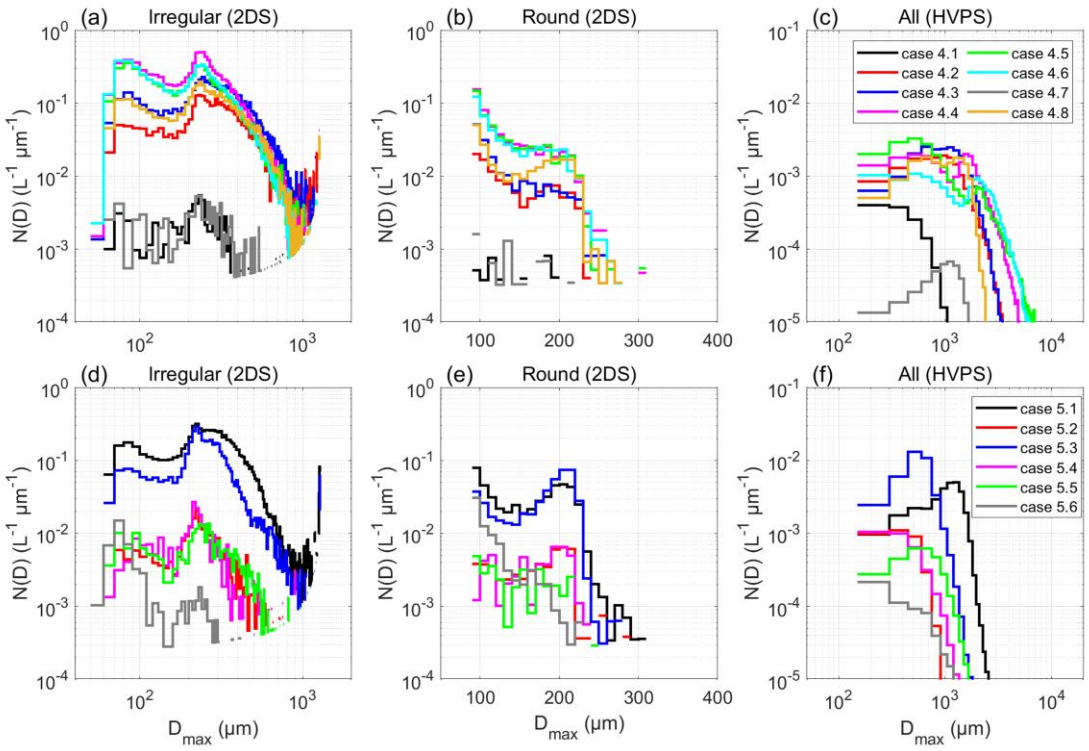

Figure 14: Mean size distributions (step plots) of ice particles (left), round droplets (drizzle, center) from 2DS and all particles(right) from HVPS: (a, b, c) case 4 and (d, e, f) case 5. Different coloured lines represent selected legs within each case.

Line 424: "clean aerosol conditions minimize competition from primary nucleation" — this is an important point. Could you elaborate on why low aerosol loading favors SIP?

Reply: We have deleted this sentence and added an explanation in Section 4.1.

Lines 543-561:

Compared with other regions, the TP convective clouds share the common HM signature between −3 and −8°C and the IMF exceeding 10000 near −4°C (N_{INP} below 0.01 L^{-1}), but they also exhibit distinct features. First, the TP combines a pristine aerosol background comparable to that of polar regions with ice concentrations comparable to those of mid-latitude and tropical convection. Aerosol particles larger than 500 nm were below 4 cm^{-3} above 6 km, and cloud droplet number concentrations over the TP are 1–2 orders of magnitude lower than those over other continental and oceanic regions (Zhao et al., 2018; Chang et al., 2019). The low droplet concentrations favor broad droplet spectra with abundant large supercooled droplets (Sect. 3.1), which provide the large droplets required by both HM and DS, whereas the scarcity of INP keeps primary ice production low. Unlike the pristine polar regions, where the absolute enhancement remains small, vigorous summer convection over the TP maintains a continuous supply of supercooled liquid water and large hydrometeors. Second, ice enhancement in case 4 extended from −3.6 to −16.3°C along a single ascent, except in downdraft regions (case 4.7). Owing to the high elevation, the 0°C level (about 5.85 km) lay only about 1.4 km above the ground at Naqu (about 4.5 km), and the updrafts spanning the 6–9 km layer (Fig. 15) could readily carry secondary ice from the HM layer to colder levels. Third, the flight-wide statistics (Fig. 16) show that strong ice enhancement occurred only where drizzle and large hydrometeors coexisted, whereas within the HM window drizzle without large ice-phase particles produced little enhancement, as in case 3. This agrees with Yang et al. (2020), who found that drizzle without significant riming could not explain the observed ice in tropical stratiform clouds, and with Lasher-Trapp et al. (2016, 2021), who emphasized the role of graupel and frozen drops retained in the HM zone. These comparisons indicate that the coexistence of large droplets and large collision partners is a general requirement for SIP, and that the TP, with its clean background and abundant supercooled liquid water, provides a natural laboratory for studying SIP in high-altitude convective clouds.